

# Record Chemical-Shift Temperature Sensitivity in a Series of Trinuclear Cobalt Complexes

Ökten Üngör, Tyler M. Ozvat, Zhen Ni, and Joseph M. Zadrozny\*



Cite This: *J. Am. Chem. Soc.* 2022, 144, 9132–9137



Read Online

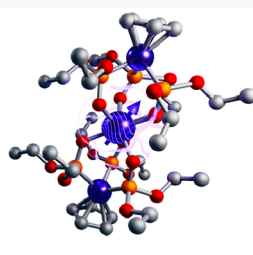
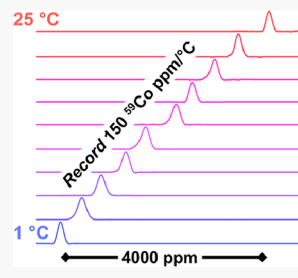
ACCESS |

Metrics & More

Article Recommendations

Supporting Information

**ABSTRACT:** Designing spins that exhibit long-lived coherence and strong temperature sensitivity is central to designing effective molecular thermometers and a fundamental challenge in the chemistry/quantum-information space. Herein, we provide a new pathway to both properties in the same molecule by designing a nuclear spin, which possesses a robust spin coherence, to mimic the strong temperature sensitivity of an electronic spin. This design strategy is demonstrated in the group of trinuclear Co(III) spin-crossover compounds  $[(\text{CpCo}(\text{OP}(\text{OR})_2)_3)_2\text{Co}](\text{SbCl}_6)$  where Cp = cyclopentadienyl and R = Me (1), Et (2), *i*-Pr (3), and *t*-Bu (4). Nuclear magnetic resonance analyses of the  $^{59}\text{Co}$  nuclear spins reveal  $^{59}\text{Co}$  chemical-shift temperature sensitivity ( $\Delta\delta/\Delta T$ ) values that span from 101(1) ppm/ $^{\circ}\text{C}$  in 1 to 149(1) ppm/ $^{\circ}\text{C}$  in 2 and 150(2) ppm/ $^{\circ}\text{C}$  in 4, where the latter two are record temperature sensitivities for any nuclear spin. Additionally, complexes 2 and 4 have  $T_2^*$  values of 74 and 78  $\mu\text{s}$  in solution at ambient temperatures surpassing those from electron-spin-based complexes, which typically display long coherence times only at extremely low temperatures. Our results suggest that spin-crossover phenomena can enable electron-spin-like temperature sensitivities in nuclear spins while retaining robust coherence times at room temperature.



## INTRODUCTION

Quantum sensing offers the possibility of developing a radically new approach to detecting chemical phenomena.<sup>1,2</sup> A central part of these efforts is the creation of quantum bits, or qubits, which are quantum objects that can exist in two states simultaneously as a superposition. The superposition states of an ideal quantum sensor are simultaneously extremely sensitive to their local environment<sup>3–5</sup> and characterized by a long lifetime,<sup>6</sup> the latter indicated by a long coherence time or  $T_2$ .<sup>a</sup>

One specific sensitivity of interest is that toward changes in temperature. Temperature-dependent magnetic resonance signals from molecular qubits could be harnessed for high-resolution noninvasive thermometry, a capability of interest in biomedical imaging.<sup>7,8</sup> Toward this application, designing highly temperature-dependent sensitivities of magnetic resonance signals, particularly in molecules, is desirable. To that end, electronic spins often have strong temperature dependences of their electron paramagnetic resonance (EPR) signals owing to changes in structure. For example, the  $S = 1$  nitrogen vacancy center in diamond has a  $T$ -dependent EPR signal from lattice expansion/contraction.<sup>1,2</sup> However, for open-shell molecules, the utility of that  $T$ -dependence is lessened owing to generally fast superposition collapse outside of  $\text{He}^{(1)}$ -temperature cryostats. Indeed, this trade off appears relatively common for spin systems—high environmental sensitivity comes at the cost of short-lived spin superpositions.

In contrast to molecular electronic spins, nuclear spins are insensitive to the environment, producing very long-lived superpositions (microseconds to milliseconds) at room

temperature and in solution. If the environmental sensitivity of these species could be designed to mimic those of open-shell systems, yet retain the relatively long coherence times, it would combine the advantages of both for quantum sensing. We note that mimicry is widespread in inorganic chemistry for, e.g., replicating the reactivity of enzymes with mononuclear metal complexes.<sup>9,10</sup> However, mimicry strategies are not yet developed to target quantum properties.

Metal complexes containing  $^{59}\text{Co}$  nuclear spins appear to be promising candidates for quantum mimicry of the temperature sensitivity of electron spins. The  $^{59}\text{Co}$  chemical shift ( $\delta$ ) and relaxation times ( $T_1$  and  $T_2$ ) are extremely sensitive to changes in local electron density, owing to the contributions to  $\delta$  from d–d excited states and to  $T_1$  and  $T_2$  from the quadrupolar  $I = 7/2$   $^{59}\text{Co}$  nucleus.<sup>11–15</sup> For these reasons, the  $^{59}\text{Co}$  nucleus has a relatively high temperature sensitivity for its chemical shift, on the order of 1–3 ppm/ $^{\circ}\text{C}$ ,<sup>16,17</sup> which is much higher than those of other prominent nuclei like  $^1\text{H}$  and  $^{19}\text{F}$ .<sup>18</sup> However, to truly mimic the temperature sensitivity of an unpaired electron's EPR signal, much higher sensitivities are necessary.

Received: March 22, 2022

Published: May 12, 2022



We propose a route to achieving even higher temperature sensitivity through coupling spin crossover, an electron-spin phenomenon, to  $^{59}\text{Co}$  NMR (Figure 1). In molecules built

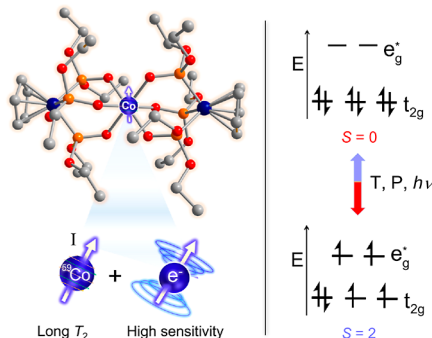


**Figure 1.** Left: The crystal structure of one of the systems of interest,  $[\text{CpCo}(\text{OP}(\text{OCH}_2\text{CH}_3)_2)_3]_2\text{Co}^+$ , taken from the previous report. H atoms are omitted for clarity. Color scheme: Co: blue, O: red, P: orange, C: gray. Right: The central blue cobalt atom is both active in the spin-crossover process and addressable via  $^{59}\text{Co}$  nuclear magnetic resonance (NMR), which enables robust coherence and high environmental sensitivity in the same species.

around this strategy, we hypothesize that the nuclear spin will mimic the temperature sensitivity of the electron spin while retaining the robust coherence of the magnetic nucleus. More specifically, we envisioned that a spin-crossover of a Co(III) ion, wherein the Co(III) shifts from a closed shell,  $S = 0$  state to a high-spin,  $S = 2$  state,<sup>19</sup> would amplify the temperature sensitivity of the  $^{59}\text{Co}$   $\delta$  through the contact shift. At the same time, we anticipated that the coherence time of the  $^{59}\text{Co}$  nuclear spin would remain long relative to an electronic spin owing to the small nuclear magnetic moment. In testing these hypotheses, we demonstrate the highest temperature sensitivity of the NMR signal for any magnetic nucleus reported to date.

## RESULTS AND DISCUSSION

**Synthesis.** For the proof of concept, we selected the complexes  $[(\text{CpCo}(\text{OP}(\text{OR})_2)_3)_2\text{Co}](\text{SbCl}_6)$  [ $\text{R} = \text{Me}$  (**1**), Et (**2**), *i*-Pr (**3**), and *t*-Bu (**4**)]. Complex **2** is the first reported example of an octahedral  $S = 0$  to  $S = 2$  spin-crossover Co(III) (Figure 1), where the central Co(III) atom undergoes a thermally induced spin crossover at room temperature.<sup>20–22</sup> Compounds **1–4** were synthesized via slight modification of literature preparations, which involves oxidizing the Co<sup>II</sup> compound  $[\text{CpCo}(\text{OP}(\text{OR})_2)_3]_2\text{Co}$  with  $[(p\text{-BrC}_6\text{H}_4)_3\text{N}]$ –(SbCl<sub>6</sub>) in CH<sub>2</sub>Cl<sub>2</sub>. The details of the syntheses can be found in the Supporting Information.

All compounds exhibit a spin crossover in the solid state as evidenced by variable-temperature magnetic susceptibility ( $\chi_M T$ ) data (Figure 2). However, the extent of the spin crossover differs. For example,  $\chi_M T$  for compound **1** varies between 0.22 and 0.55 cm<sup>3</sup> K/mol from 5 to 330 K, indicating a predominantly low-spin (expected  $\sim 0$  cm<sup>3</sup> K/mol for  $S = 0$ ) and either a remnant high-spin population or significant temperature-independent paramagnetism (TIP). At the very highest temperatures of measurement,  $\chi_M T$  for **1** has an upward inflection, likely signifying spin crossover beyond the measurement window. Compounds **2** and **4** are similar but show an onset of the spin crossover at a lower temperature than **1**. Furthermore, there is a greater contribution of either high-spin fractions or TIP to the  $\chi_M T$  data for **2** and **4**, as

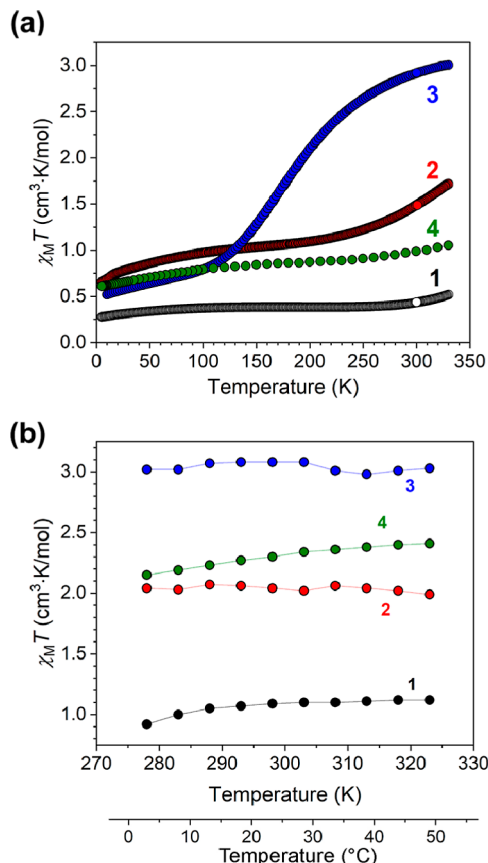


**Figure 2.** (a) Temperature dependence of the magnetic susceptibility of polycrystalline samples of **1–4**. (b) Solution-phase measurements of magnetic susceptibility  $\chi_M T$  vs  $T$  for **1–4** in CDCl<sub>3</sub> solution, from 273 to 325 K, in intervals of 5 K, by Evans' method (see the text and the Supporting Information for details).

evidenced by the higher  $\chi_M T$  values (ca. 0.55 cm<sup>3</sup> K/mol) at low temperatures. The spin crossovers are therefore incomplete for **1**, **2**, and **4**. Complex **3**, in contrast, undergoes a complete spin transition at ca. 170 K with no hysteresis. The  $\chi_M T$  value of ca. 3.3 cm<sup>3</sup> K/mol observed at room temperature agrees with the expected values for high-spin  $S = 2$  ions (3.00 cm<sup>3</sup> K/mol with  $g = 2.00$ ).

In solution, complexes **1–4** exhibit ranging extents of the spin crossover near room temperature. Evans' method<sup>23,24</sup> was used to determine the magnetic susceptibility of **1**, **2**, and **4** in 15 mM CDCl<sub>3</sub> solution in the temperature range of 275–325 K (Figures 2b, S1–S4), here limited by the freezing and boiling points of CDCl<sub>3</sub>. The  $\chi_M T$  values for **2** and **3** are consistent with the data obtained from solid-state magnetic measurements. For **2**, the  $\chi_M T$  value remains constant at ca. 2 cm<sup>3</sup> K/mol, corresponding to  $\sim 60\%$  of the high-spin (HS) state. The  $\chi_M T$  value for complex **3** also remains constant with the value of ca. 3 cm<sup>3</sup> K/mol, in agreement with the HS behavior observed in the solid-state measurements. A stronger-field ligand generally imparts a higher-temperature crossover and lower % conversion near room temperature for a spin-crossover ion.<sup>25</sup> Thus, both the solution and solid-state  $\chi_M T$  data suggest the following trend in central Co(III) ligand field strength with ligand R groups: Me < Et < *t*-Bu < *i*-Pr. These results are in agreement with the previously recorded solid-state magnetic measurements.<sup>21</sup> We note that the temperature dependence of the magnetic moment in solutions differs from

the measurements on the polycrystalline samples. One factor that governs the spin-crossover behavior in the solid state is cooperativity between spin-crossover centers,<sup>19</sup> and cooperativity is completely negated in solutions. Furthermore, the different chemical environment around the molecules in solution versus the solid state likely alters the effective ligand field, also shifting the spin crossover transition temperature. These two factors may explain the relative difference in the two data sets. We also note the relatively small temperature window over which Evans' method was performed, which would similarly lead to a relatively small change in magnetic moment.

Variable-temperature <sup>59</sup>Co nuclear magnetic resonance (NMR) spectra at ca. 118.67 MHz were collected on 400 mM solutions of **1**, **2**, and **4** in CH<sub>2</sub>Cl<sub>2</sub> from 0 to 25 °C (Figures 3, S5 and S6) in the 11.74 T magnet of a "500 MHz"

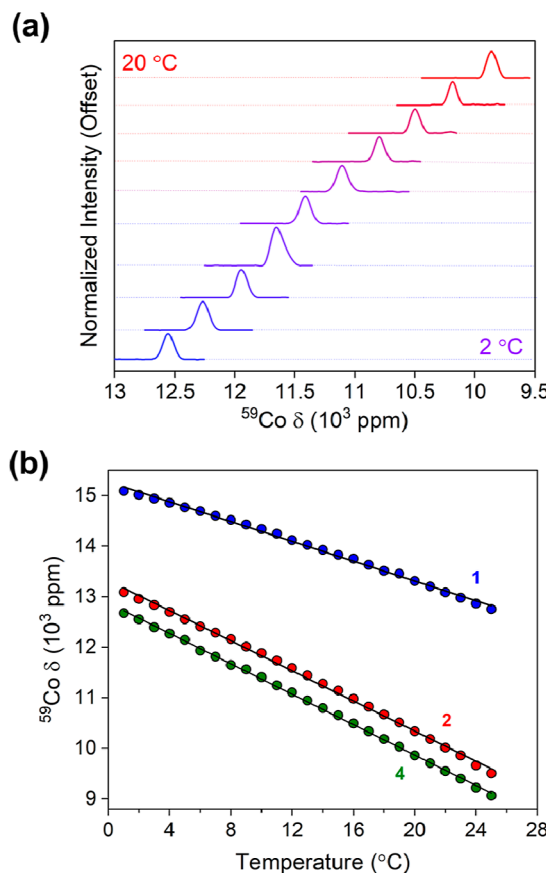


**Figure 3.** (a) Temperature dependence of the chemical shift of **4** (<sup>59</sup>Co NMR at 118.67 MHz in CH<sub>2</sub>Cl<sub>2</sub>) is shown through spectra collected at incremental temperatures with steps of 2 °C. The dashed lines are added to visualize the baseline for each spectrum, but the windows of collection are indicated by the continuous data sets. The system was allowed to equilibrate for 5 min between each temperature point before each measurement. (b) Chemical shift values for **1**, **2**, and **4** as a function of temperature. The solid black lines are the result of linear fits.

NMR. Attempts to locate a peak for the fully open-shell complex **3** were unsuccessful. The NMR spectra for **1**, **2**, and **4** reveal a broad <sup>59</sup>Co peak with dramatic upfield shifts with increasing temperature. For example, for **1**, the peak shifts from 15 000 to ca. 13 000 ppm over this 25 °C interval. Compounds **2** and **4** shift by much larger amounts, from ca. 13 000 to 9000

ppm. Linear regression of the temperature dependence of the <sup>59</sup>Co chemical shifts yielded values of 101(1), 149(1), and 150(2) ppm/°C for **1**, **2**, and **4**, respectively. To the best of our knowledge, these are the highest chemical-shift temperature sensitivities for any nucleus. Finally, we note that there is also an additional peak in the spectra from the <sup>121</sup>Sb nucleus (ca. 120 MHz at 11.74 T) of the SbCl<sub>6</sub><sup>-</sup> anion in the range of 9000–8000 ppm<sup>18</sup> above 20 °C (Figure S7); however, in contrast to the <sup>59</sup>Co peak, <sup>121</sup>Sb is relatively temperature-insensitive (<1.0 ppm/°C) and much sharper [full width at half-maximum (FWHM) = 1.5 ppm, or ~178 Hz].

<sup>59</sup>Co NMR linewidths contain information about the relaxation time  $T_2^*$ , the dephasing time of the nuclear spin, which is a proxy for the coherence time. The <sup>59</sup>Co NMR peaks for **1**, **2**, and **4** are all very broad (FWHM of 86, 165, and 137 ppm for **1**, **2**, and **4**, respectively at 0 °C) and decrease with increasing temperature for **2** and **4** but increase with increasing temperature for **1**. Linewidth ( $\nu_{1/2}$ ) values extracted from Lorentzian fits of the resonance peaks reflect this trend (Figure 4a), decreasing with increasing temperature in complex **1** but

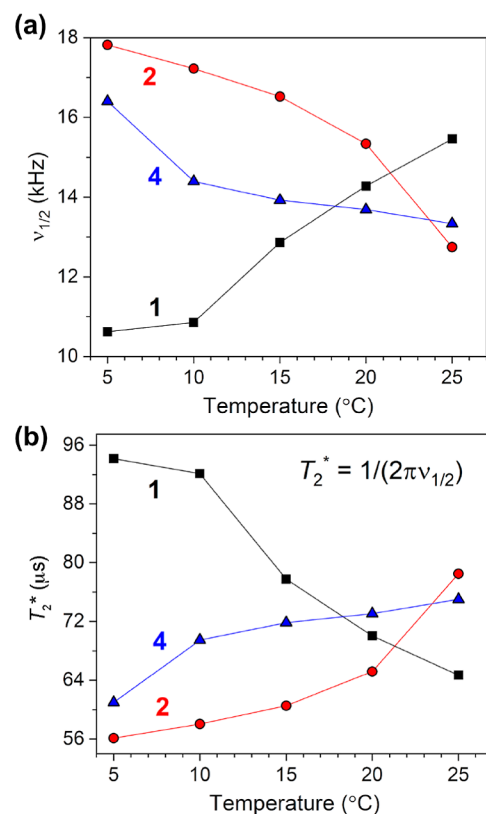


**Figure 4.** (a) <sup>59</sup>Co NMR linewidth values for **1**, **2**, and **4** as a function of temperature. The solid black lines are the result of a linear fit. (b) Temperature dependence of  $T_2^*$  values for **1**, **2**, and **4** calculated using the resonance linewidths.

increasing with increasing temperature for complexes **2** and **4**. Values of  $T_2^*$  were extracted from the temperature-dependent NMR linewidths through the relationship  $T_2^* = 1/(2\pi\nu_{1/2})$  where  $\nu_{1/2}$  (Hz) is the linewidth (at FWHM) of the <sup>59</sup>Co-NMR peak. At 25 °C, the  $T_2^*$  values for complexes **2** and **4** are 78 and 74  $\mu$ s, respectively (Figure 4b), and they both slightly decrease with temperature. In contrast, the  $T_2^*$  value for **1** is slightly shorter, 65  $\mu$ s at room temperature, and it increases as the temperature decreases. An exact mechanistic under-

standing of these trends is currently elusive, likely needing a comprehensive model featuring changes in  $T_1$ , correlation time, and the spin crossover. The most important takeaway of these data is that the magnitude remains quite long, ca. 50–100  $\mu$ s, over the studied temperature window.

The second  $^{59}\text{Co}$  nuclear-spin-relaxation property we investigated was the spin-lattice relaxation time,  $T_1$ , for these complexes. Variable-temperature inversion recovery experiments were performed on **1** and attempted for **2** and **4** over the 5–25 °C temperature range. In these experiments, the peak height of **1** was affected (Figure S8); the peak dipped in intensity shortly after the inverting pulse and recovered, but the power of our instrument never fully inverted the population. This observation was especially true for **2** and **4**, which did not exhibit a change in peak intensity with any length of the inversion pulse, likely because  $T_1$  for these is below the minimum range accessible with our instrument (see the Supporting Information). The data for **1** showed a slight lengthening of  $T_1$  with decreasing temperature. At 25 °C, the  $T_1$  value for **1** was calculated as 52  $\mu$ s, and it increased to 58  $\mu$ s at 5 °C. The general magnitudes of these values are consistent with other  $^{59}\text{Co}$  relaxation studies of Co(III) complexes.<sup>26,27</sup>

Finally, we tested the matrix sensitivity of the  $^{59}\text{Co}$  NMR response in the form of variable-concentration and variable-solvent studies. Variable-temperature  $^{59}\text{Co}$  signals were collected on **1** and **2** with concentrations of 50, 100, and 400 mM (for **1**) and 100, 200, 300, and 400 mM (for **2**). In both complexes, the concentration dependence of the chemical shift was negligible (Figures S9 and S10) as was the temperature sensitivity. In addition, the solvent dependencies of the chemical shifts of **1** and **2** were tested in  $\text{CH}_2\text{Cl}_2$ ,  $\text{CHCl}_3$ , and  $\text{CDCl}_3$  (Figures S11 and S12). The resonance line and its temperature dependence remained constant in  $\text{CHCl}_3$  and  $\text{CDCl}_3$ , suggesting minimal impact from solvent deuteration. In contrast, the  $^{59}\text{Co}$  NMR spectra shifted nearly 20 ppm when samples were dissolved in  $\text{CH}_2\text{Cl}_2$ , but the temperature dependence remained the same at  $\text{CHCl}_3$ . In principle, the higher concentrations of spin-crossover ions and changes in solvent viscosity should be expected to affect the relaxation times and therefore linewidths. It is therefore remarkable that no solvent or concentration dependence of the linewidth was found in these studies, underlining the robustness of the  $^{59}\text{Co}$  nuclear spin coherence.

The foregoing data are important for two main reasons related to the magnitude of the temperature dependence of the  $^{59}\text{Co}$  chemical shift and the observed  $T_2^*$  times. First, to the best of our knowledge, the ca. 150 ppm/°C  $\Delta\delta/\Delta T$  for the  $^{59}\text{Co}$  nucleus is larger than all other reported systems, many by at least an order of magnitude (Figure 5). For example, the typical temperature dependence of the  $^{59}\text{Co}$  NMR shift is between 1 and 3 ppm/°C, with the highest for a Co(III) complex belonging to  $[\text{Co}(\text{acac})_3]$  (acac = acetylacetone) at 3.15 ppm/°C.<sup>17,28</sup> Relatively recently, a higher temperature dependence was reported for a putative Co(II) complex at 8.5 ppm/°C.<sup>29</sup> The complexes here eclipse all of those. A preliminary study of **2** in a 300 MHz NMR showed 131 ppm/°C—and our results here, which are even higher, suggest amplification of  $T$  sensitivity with the higher magnetic field.<sup>20</sup>

There are other systems that exploit electronic-spin phenomena to affect  $T$ -dependent NMR properties, but they are all surpassed by **1**, **2**, and **4**. For example, the spin-crossover of Fe(II) complexes is applied to shifting ligand-based  $^{19}\text{F}$  nuclei, but the sensitivities are relatively small (0.7 ppm/°C).<sup>30</sup>

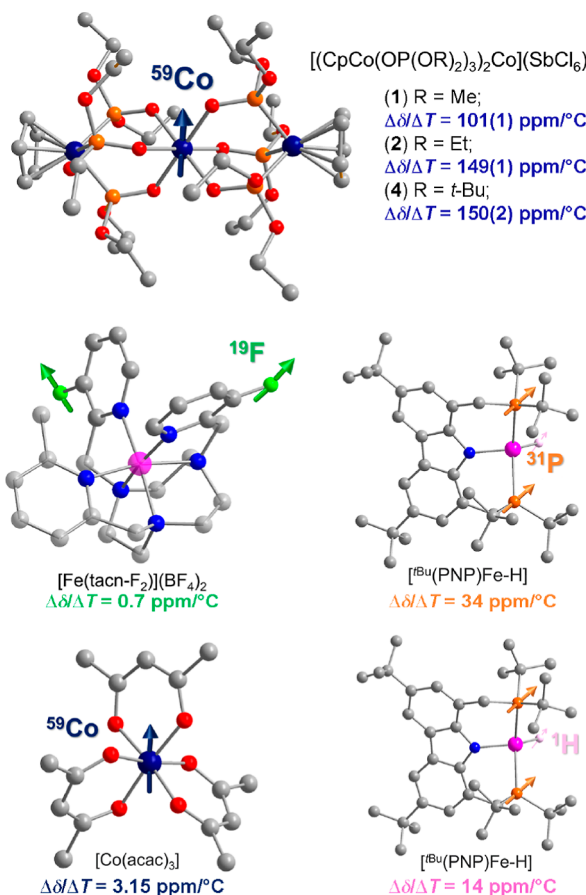


**Figure 5.** Visual comparison of the sensitivity of  $\delta$  to temperature of **1**, **2** and **4** with  $^{59}\text{Co}$  and other notable nuclei. Data were extracted from refs 17, 30–32. Conditions under which these data were collected follow  $[\text{Co}(\text{acac})_3]$ : 0.1 M in  $\text{C}_6\text{D}_6$  (65 MHz);  $^{19}\text{F}$ -Fe: 2.1 M in  $\text{H}_2\text{O}$  (400 MHz);  $^1\text{H}$ -[ $^{t}\text{Bu}$ (PNP)FeH]: toluene- $d_8$  (400 MHz);  $^{31}\text{P}$ -[ $^{t}\text{Bu}$ (PNP)FeH]: toluene- $d_8$  (200 MHz).

Separately, a recent pair of studies on  $^1\text{H}$  and  $^{31}\text{P}$  nuclei coordinated to Fe(III) exhibited a huge change in thermal sensitivities of the  $^1\text{H}$  and  $^{31}\text{P}$  chemical shifts,<sup>31,32</sup> 14 and 34 ppm/°C, respectively. In both these cases, interactions between the nuclei and the paramagnetic (or spin-crossover) ion are primarily through the pseudo-contact shift and Fermi contact contributions,<sup>33–35</sup> the latter less important when the nucleus of interest is spaced far from the metal ion. The direction of the chemical shift changes in these paramagnetic complexes then follows the temperature dependence of these interactions.<sup>36</sup> Complexes **1**, **2**, and **4** present a unique case where the nucleus spin and the electron spin are located on the same atom. As a result, the Fermi contact part of the hyperfine coupling becomes very large, and the temperature dependence of this term is likely directing the enormous  $\Delta\delta/\Delta T$  values. We anticipate that this approach of co-localization of the two interacting spins to the same atom will produce future compounds with additional strong environmental sensitivities.

Comparison of the temperature dependence of the  $^{59}\text{Co}$  NMR signal for **1**–**4** with the temperature dependence of electronic spins reveals how substantial the changes are. For example, the most popular current thermometer for quantum sensing applications is the  $S = 1$ , open-shell nitrogen-vacancy center in diamond. Owing to changes in the lattice with changes in temperature, the  $S = 1$  color center has a change in

its zero-field splitting parameter, which changes the EPR frequency by  $78 \text{ kHz}/^\circ\text{C}$ .<sup>37,38</sup> At 118.67 MHz (11.74 T), the 150 ppm/°C change of **2** corresponds to an 18 kHz/°C change in the <sup>59</sup>Co NMR resonant frequency, which is on the same order of magnitude as the electron spin. Hence, the nuclear spin here exhibits a temperature dependence that mimics that of an electron spin, driven by the spin-crossover phenomena of the Co(III) ion in which the <sup>59</sup>Co nucleus is housed. Thus, we have a set of compounds that are true quantum mimics—nuclear spins behaving like electronic spins.

Another remarkable facet of the studied complexes are the relatively long dephasing times for the nuclear spin. At ca. 70  $\mu\text{s}$ , the observed dephasing times are on par with the desired 100  $\mu\text{s}$  target for applicability of electronic spins in quantum computing applications but shorter than the highest value observed so far for a metal complex: 0.7 ms for the  $S = 1/2$  [V (C<sub>8</sub>S<sub>8</sub>)<sub>3</sub>]<sup>2-</sup>.<sup>39</sup> However, we note that the latter observations are made at low temperatures, under extremely dilute conditions (<0.1 mM), and in frozen solids engineered to be devoid of magnetically noisy nuclear spins. Our relaxation times here are recorded at a high concentration (400 mM), above room temperature, and in dynamic fluid environments full of <sup>1</sup>H and <sup>2</sup>H magnetic nuclei. The robustness of the coherence is even more remarkable considering that it does not change with the increasing concentration of the spin-crossover units, which would be expected to bring more magnetic noise to the environment and engender even shorter dephasing times. Finally, we note that some aspects of the linewidths observed may be due to some temperature inhomogeneity in the sample, and thus the  $T_2^*$  values reported here should be considered only as the lower bound of their true values.

## CONCLUSIONS

The foregoing data present record chemical-shift temperature sensitivities for any nuclear spin. The sensitivities are driven by the effect of spin crossover, which enables a <sup>59</sup>Co nuclear spin to mimic the thermometry capabilities of an electron spin. The results also show that the extent of mimicry is tunable, as the temperature sensitivity differs depending on the chosen R group in the presented complexes. We note that there are many more properties where a nuclear spin mimic of an electron spin may be advantageous to quantum applications; for example, boosting the spin polarization of nuclear spins to match those of electrons, which would enable high-signal-to-noise sensing from a long-lived superposition, an important goal for quantum sensing applications.<sup>40</sup> Furthermore, there are many other spin-change phenomena in metal complexes (e.g. valence tautomerization<sup>41</sup>) and with other magnetic metal nuclei, which may reveal similarly very strong temperature-dependent NMR signals. Ongoing efforts in these areas will be reported in due course.

## ASSOCIATED CONTENT

### Supporting Information

The Supporting Information is available free of charge at <https://pubs.acs.org/doi/10.1021/jacs.2c03115>.

Additional experimental and sample preparation details, magnetic data, and magnetic resonance characterization (PDF)

## AUTHOR INFORMATION

### Corresponding Author

Joseph M. Zadrozny – Department of Chemistry, Colorado State University, Fort Collins, Colorado 80523, United States;  [orcid.org/0000-0002-1309-6545](https://orcid.org/0000-0002-1309-6545); Email: [Joe.Zadrozny@colostate.edu](mailto:Joe.Zadrozny@colostate.edu)

### Authors

Ökten Üngör – Department of Chemistry, Colorado State University, Fort Collins, Colorado 80523, United States  
Tyler M. Ozvat – Department of Chemistry, Colorado State University, Fort Collins, Colorado 80523, United States  
Zhen Ni – Department of Chemistry, Texas A&M University, College Station, Texas 77843, United States;  [orcid.org/0000-0002-8216-3748](https://orcid.org/0000-0002-8216-3748)

Complete contact information is available at: <https://pubs.acs.org/10.1021/jacs.2c03115>

### Notes

The authors declare no competing financial interest.

## ACKNOWLEDGMENTS

This work was supported by the National Science Foundation (NSF) via awards NSF-1465954 and Colorado State University. Magnetometry, NMR, and standard molecular characterization were performed at the Colorado State University Analytical Resources Core Facility RRID:SCR\_021758, which is supported by an NIH-SIG award (1S10OD021814-01) and the CSU-CORES Program. We also thank Dr. Chung-Jui Yu for graphical assistance.

## ADDITIONAL NOTE

<sup>a</sup>The coherence time of a spin is also known as the spin–spin relaxation time,  $T_2$ , in the NMR and EPR fields.

## REFERENCES

- (1) Yang, M.; Yuan, Q.; Gao, J.; Shu, S.; Chen, F.; Sun, H.; Nishimura, K.; Wang, S.; Yi, J.; Lin, C.-T.; Jiang, N. A diamond temperature sensor based on the energy level shift of nitrogen-vacancy color centers. *J. Nanomater.* **2019**, *9*, 1576.
- (2) Wu, Y.; Weil, T. Recent developments of nanodiamond quantum sensors for biological applications. *Adv. Sci.* **2022**, *9*, No. e2200059.
- (3) Yu, C.-J.; von Kugelgen, S.; Laorenza, D. W.; Freedman, D. E. A molecular approach to quantum sensing. *ACS Cent. Sci.* **2021**, *7*, 712–723.
- (4) Poggiali, F.; Cappellaro, P.; Fabbri, N. Optimal control for one-qubit quantum sensing. *Phys. Rev. X* **2018**, *8*, 021059.
- (5) Gefen, T.; Rotem, A.; Retzker, A. Overcoming resolution limits with quantum sensing. *Nat. Commun.* **2019**, *10*, 4992.
- (6) Degen, C. L.; Reinhard, F.; Cappellaro, P. Quantum sensing. *Rev. Mod. Phys.* **2017**, *89*, 035002.
- (7) Rieke, V.; Butts Pauly, K. MR thermometry. *J. Magn. Reson. Imaging* **2008**, *27*, 376–390.
- (8) Townsend, D.; Cheng, Z.; Georg, D.; Drexler, W.; Moser, E. Grand challenges in biomedical physics. *Front. Phys.* **2013**, *1*, 1–6.
- (9) Cook, S. A.; Hill, E. A.; Borovik, A. S. Lessons from Nature: A bio-inspired approach to molecular design. *Biochem.* **2015**, *54*, 4167–4180.
- (10) Lyu, Y.; Scrimin, P. Mimicking Enzymes: The quest for powerful catalysts from simple molecules to nanozymes. *ACS Catal.* **2021**, *11*, 11501–11509.
- (11) Yamasaki, A. Cobalt-59 nuclear magnetic resonance spectroscopy in coordination chemistry. *J. Coord. Chem.* **1991**, *24*, 211–260.

(12) Freeman, R.; Murray, G. R.; Richards, R. E. Cobalt nuclear resonance spectra. *Proc. R. Soc. A: Math. Phys. Eng. Sci.* **1957**, *242*, 455–466.

(13) Kidd, R. G. Nuclear shielding of the transition metals. *Annu. Rep. NMR Spectrosc.* **1980**, *10*, 1–79.

(14) Glemann, G.; Lever, A. B. P. *Inorganic Electronic Spectroscopy: Studies in Physical and Theoretical Chemistry*; Press Elsevier, 1984; pp 86–130.

(15) Bramley, R.; Brorson, M.; Sargeson, A. M.; Schaeffer, C. E. Cobalt-59 NMR chemical shifts of cobalt(III) complexes; correlations with parameters calculated from ligand-field spectra. *J. Am. Chem. Soc.* **2002**, *107*, 2780–2787.

(16) Benedek, G. B.; Englman, R.; Armstrong, J. A. Temperature and pressure dependence of the Co59 nuclear resonance chemical shift. *J. Chem. Phys.* **1963**, *39*, 3349–3363.

(17) Levy, G. C.; Terry Bailey, J.; Wright, D. A. A sensitive NMR thermometer for multinuclei FT NMR. *J. Magn. Reson.* **1980**, *37*, 353–356.

(18) Harris, R. K. N.m.r. and the periodic table. *Chem. Soc. Rev.* **1976**, *5*, 1–22.

(19) Gütlich, P.; Goodwin, H. A. *Spin Crossover in Transition Metal Compounds I*; Topics in Current Chemistry; Springer: Berlin/Heidelberg, 2004; pp 1–47.

(20) Navon, G.; Klaeui, W. Cobalt-59 NMR of a cobalt(III) spin-crossover compound. *Inorg. Chem.* **1984**, *23*, 2722–2725.

(21) Klaeui, W.; Eberspach, W.; Guetlich, P. Spin-crossover cobalt(III) complexes: steric and electronic control of spin state. *Inorg. Chem.* **1987**, *26*, 3977–3982.

(22) Goodwin, H. A. *Spin Crossover in Transition Metal Compounds II*; Topics in Current Chemistry; Springer: Berlin/Heidelberg, 2004; pp 49–62.

(23) Evans, D. F. 400. The determination of the paramagnetic susceptibility of substances in solution by nuclear magnetic resonance. *J. Chem. Soc.* **1959**, 2003–2005.

(24) Schubert, E. M. Utilizing the Evans method with a superconducting NMR spectrometer in the undergraduate laboratory. *J. Chem. Educ.* **1992**, *69*, 62.

(25) Hauser, A. Ligand field theoretical considerations. *Top. Curr. Chem.* **2004**, *233*, 49–58.

(26) Kirby, C. W.; Puranda, C. M.; Power, W. P. Cobalt-59 nuclear magnetic relaxation studies of aqueous octahedral cobalt(III) complexes. *J. Phys. Chem.* **1996**, *100*, 14618–14624.

(27) Ader, R.; Loewenstein, A. Nuclear magnetic relaxation studies in solutions of symmetric cobalt (III) complexes. *J. Magn. Reson.* **1971**, *5*, 248–261.

(28) Au-Yeung, S. C. F.; Eaton, D. R. The solvent and field dependence of 59Co NMR linewidths. *J. Magn. Reson.* **1983**, *52*, 366–373.

(29) Billeci, F.; Gunaratne, H. Q. N.; Licence, P.; Seddon, K. R.; Plechkova, N. V.; D'Anna, F. Ionic liquids–cobalt(II) thermochromic complexes: how the structure tunability affects “self-contained” systems. *ACS Sustainable Chem. Eng.* **2021**, *9*, 4064–4075.

(30) Thorarinsdottir, A. E.; Gaudette, A. I.; Harris, T. D. Spin-crossover and high-spin iron(ii) complexes as chemical shift (19)F magnetic resonance thermometers. *Chem. Sci.* **2017**, *8*, 2448–2456.

(31) Ott, J. C.; Wadeohl, H.; Enders, M.; Gade, L. H. Taking solution proton NMR to its extreme: prediction and detection of a hydride resonance in an intermediate-spin iron complex. *J. Am. Chem. Soc.* **2018**, *140*, 17413–17417.

(32) Ott, J. C.; Suturina, E. A.; Kuprov, I.; Nehrkorn, J.; Schnegg, A.; Enders, M.; Gade, L. H. Observability of paramagnetic NMR signals at over 10 000 ppm chemical shifts. *Angew. Chem., Int. Ed.* **2021**, *60*, 22856–22864.

(33) Soliverez, C. E. The contact hyperfine interaction: an ill-defined problem. *J. Phys. C: Solid State Phys.* **1980**, *13*, L1017–L1019.

(34) Bucher, M. The electron inside the nucleus: an almost classical derivation of the isotropic hyperfine interaction. *Eur. J. Phys.* **2000**, *21*, 19–22.

(35) Blahut, J.; Benda, L.; Kotek, J.; Pintacuda, G.; Hermann, P. Paramagnetic cobalt(II) complexes with cyclam derivatives: toward (19)F MRI contrast agents. *Inorg. Chem.* **2020**, *59*, 10071–10082.

(36) Parigi, G.; Luchinat, C. Chapter 1. NMR consequences of the nucleus–electron spin interactions. *J. Biomol. NMR* **2018**, *16*, 1–41.

(37) Felton, S.; Edmonds, A. M.; Newton, M. E.; Martineau, P. M.; Fisher, D.; Twitchen, D. J. Electron paramagnetic resonance studies of the neutral nitrogen vacancy in diamond. *Phys. Rev. B: Condens. Matter Mater. Phys.* **2008**, *77*, No. 081201(R).

(38) Simpson, D. A.; Ryan, R. G.; Hall, L. T.; Panchenko, E.; Drew, S. C.; Petrou, S.; Donnelly, P. S.; Mulvaney, P.; Hollenberg, L. C. L. Electron paramagnetic resonance microscopy using spins in diamond under ambient conditions. *Nat. Commun.* **2017**, *8*, 458.

(39) Zadrozny, J. M.; Niklas, J.; Poluektov, O. G.; Freedman, D. E. Millisecond coherence time in a tunable molecular electronic spin qubit. *ACS Cent. Sci.* **2015**, *1*, 488–492.

(40) Corzilius, B.; Michaelis, V. K.; Penzel, S. A.; Ravera, E.; Smith, A. A.; Luchinat, C.; Griffin, R. G. Dynamic nuclear polarization of (1)H, (13)C, and (59)Co in a tris(ethylenediamine)cobalt(III) crystalline lattice doped with Cr(III). *J. Am. Chem. Soc.* **2014**, *136*, 11716–11727.

(41) Beni, A.; Dei, A.; Laschi, S.; Rizzitano, M.; Sorace, L. Tuning the charge distribution and photoswitchable properties of cobalt-dioxolene complexes by using molecular techniques. *Chem. Eur. J.* **2008**, *14*, 1804–1813.

## □ Recommended by ACS

### Designing Magnetic Superalkalis with Extremely Large Nonlinear Optical Responses

Wei-Ming Sun, Xiang-Hui Li, et al.

AUGUST 15, 2022  
ORGANOMETALLICS

READ ▶

### Cooperative Spin Crossover above Room Temperature in the Iron(II) Cyanoborohydride–Pyrazine Complex

Yuriii S. Bibik, Il'ya A. Gural'skiy, et al.

SEPTEMBER 06, 2022  
INORGANIC CHEMISTRY

READ ▶

### Redox-Responsive MRI Probes Based on First-Row Transition-Metal Complexes

Janet R. Morrow, Priya Ranjan Sahoo, et al.

SEPTEMBER 06, 2022  
INORGANIC CHEMISTRY

READ ▶

### 105 K Wide Room Temperature Spin Transition Memory Due to a Supramolecular Latch Mechanism

Maksym Seredyuk, José Antonio Real, et al.

JULY 28, 2022  
JOURNAL OF THE AMERICAN CHEMICAL SOCIETY

READ ▶

Get More Suggestions >